Multinuclear Clusters of Manganese and Lithium with Silsesquioxane-derived Ligands: Synthesis and Ligand Rearrangement by Dioxygen- and Base-mediated Si-O Bond Cleavage

Michael R. Gau,† Michael J. Zdilla*

Department of Chemistry, Temple University, 1901 N. 13th St., Philadelphia, PA 19122

Manganese Clusters, Oxygen Evolving Complex, POSS, Oxygen Activation

ABSTRACT: Synthesis of manganese cluster complexes templated by polyhedral oligomeric silsesquioxane (POSS)-derived ligands is described. $Mn^{II}_3(Ph_7Si_7O_{12})_2Pyr_4$ (**1**), and $Mn^{II}_4(Ph_4Si_4O_8)_2(Bpy)_2(Py)_2$ (**3**) are prepared by replacement of the amide ligands of $Mn(NR_2)_2$ (R = $SiMe_3$) via ligand protolysis by the acidic proton of the respective silsesquioxane-derived silanols. Complex **1** is shown to undergo ligand rearrangement by reaction with O_2, which results in oxidation of the cluster to a mixed $Mn^{II/III}$ cluster, concomitant with cleavage of the Si-O bonds of the ligand, releasing a $[Ph_2Si\text{-}O]^+$ unit, opening a new ligating siloxide group, and resulting in the formation of $Mn_3(Ph_6Si_6O_{11})_2Pyr_4$ (**2**). The ligand framework of **1** can also be perturbed by base. Addition of LiOH/BuLi delivers a soluble equivalent of Li_2O to **1**, resulting in cleavage of Si-O bonds, and linkage of the resulting exposed silicon atoms by the new oxide, giving a linked ligand variant that templates a Li_2Mn_3 cluster, $Mn_3Li_2(Ph_7Si_7O_{12}OPh_7Si_7O_{12})DMF_5Pyr$ (**4**). These systems are characterized by single-crystal X-ray diffraction, absorption spectroscopy, FTIR, Cyclic Voltammetry, and CHN combustion analysis. Mechanistic implications for the Si-O bond cleavage events are discussed.

Polyhedral oligomeric silsesquioxane (POSS) and related compounds have sparked new hybrid organic/inorganic nanomaterials studies due to their organic-inorganic hybrid composition and ability to mediate mixing of nanoparticles with polymers.[1] POSS-derived compounds have been examined as models for catalytic oxide surfaces[2,3] and for the syntheses of new catalysts.[4-8] Multidentate oxo-containing ligands are of interest as models of mineral surfaces, and can give rise to catalytic chemistry that is more easily scrutable than those occurring at defect active sites of bulk materials.[9,10]

The most utilized strategy of linking metal species to the silsesquioxane compounds is to use partially condensed silsesquioxane alcohols, which allow for protolysis of the hydroxyl groups and has been previously reported in synthesis of a variety of metal silsesquioxanes. A search of the Cambridge Crystal Structure Database (CSD)[11] reveals more than a hundred transition metal complexes, though only a few examples with manganese.[3,12] A study by Lorenz et al. describes the synthesis of heterometallic silsesquioxane-derived clusters using $Na(N(SiMe_3)_2)$, $Li(N(SiMe_3)_2)$, $MnCl_2$ and $(c\text{-}C_6H_{11})_7Si_7O_9(OH)_3$ resulting in $Mn_2Na_2L_2$ and $Mn_4Li_2L_2$ compounds, but the reactivity of these clusters was not further discussed.[12] In another study from Riollet et al, the silsesquioxane ligand was studied as a model of a silica-surface-templated active heterogeneous catalytic species.[3] Among other first-row *d*-block metal complexes of silsequioxanes, Ti,[13-24] Fe,[25-31] V,[32-37] and Zn[31,38-40] are most common, though there are examples with Co,[41-45] Cr,[37,46,47] Cu,[40,48-52] and one with Sc.[53] We report here the synthesis of multinuclear Mn complexes of POSS-derived ligands via reaction of $Mn(N(SiMe_3)_2)_2$ and 1,3,5,7,9,11,14-heptaphenyl-2,4,6,8,10,12,13,15,16-nonaoxa-1,3,5,7,9,11,14-heptasilatricyclo[7.3.3.15,11]hexadecane-3,7,14-triol ($Ph_7Si_7O_9(OH)_3$, $(L1)H_3$) and (2s,4s,6s,8s)-2,4,6,8-tetraphenyl-1,3,5,7,2,4,6,8-tetraoxatetrasilocane-2,4,6,8-tetraol ($Ph_4Si_4O_4(OH)_4$,, $(L2)H_4$). Ligands L1 and L2 are illustrated in Scheme 1. L2 is an unusual silsesquioxane template, with only three structural reports of coordination complexes to our knowledge.[24,45,54] The L1 ligand scaffold is much more common, representing the templating ligand for the manganese chemistry of Lorenz et al.,[12] as well as four other reports of complexes of 1st row transition metals.[32,33,38,42] We additionally present rearrangement chemistry of ligand L1 involving Si-O bond cleavage reactions mediated by O_2 and by hydroxide.

Reaction of $Mn(NR_2)_2$[55] with $(L1)H_3$ results in a colorless crystalline compound with the formula, $Mn_3(Ph_7Si_7O_{12})_2Pyr_4$ (**1**), isolated in good yield (Scheme 1). The product was identified with single crystal X-ray diffraction (Figure 1) and is pure based on CHN combustion analysis.

The crystal structure of **1** reveals an asymmetric trinuclear metal complex with each of the Mn metal centers having unique ligand environments (Figure 1), and a cluster structure that is unique to silsesquioxane systems based on a search of the CSD.[11] Each L1 pro-ligand $(L1)H_3$ provides two μ-oxygen bridges and a terminal oxygen ligand. Mn(2) has a pseudotetrahedral geometry and is coordinated by a terminal pyridine, a terminal silsesquioxane oxygen ligand,

and two μ-oxygen atoms to Mn(1) and Mn(3). Mn(1) is a five-coordinate metal center that is bound by two terminal pyridine molecules and three bridging μ-oxygen atoms (two μ-oxygen to Mn(3) and one μ-oxygen to Mn(2)). Mn(3) is another five-coordinate metal center that is ligated by a terminal pyridine, one terminal siloxide-O atom, and two μ-oxygen bridges to Mn(1) and one μ-oxygen to Mn(2). In addition, the rhomb that is formed between Mn(1), Mn(3), and the corresponding μ-oxygen bridges from separate L1 cages display different bond lengths (see Table S2).

Scheme 1.

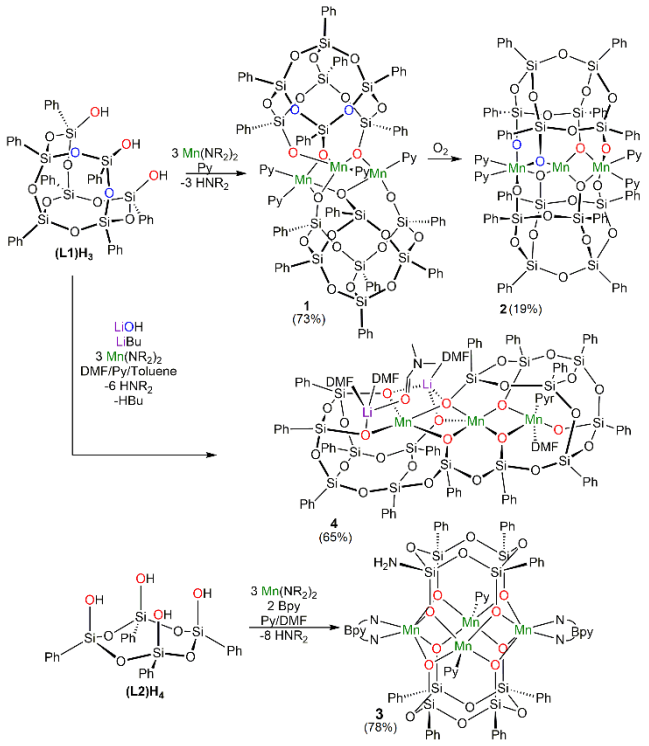

Due to the paramagnetic nature of **1**, ^{1}H NMR spectroscopy did not reveal any assignable resonances. UV/visible spectroscopy of **1** in THF only shows a small shoulder peak at 315 nm and a large charge transfer band that tails into the UV region. The lack of *d-d* transition supports a Mn^{II} oxidation state assignment. Cyclic voltammetry reveals a reversible oxidation wave at 0.172 V vs Fc as well as an irreversible reduction at -2.04 V vs Fc (Figure S1).

Complex **1** is air sensitive, changing color from colorless to dark purple upon exposure to oxygen. The resulting UV/visible spectrum displays an overall increase in absorbance with a small peak at 450 nm, which we attribute to a *d-d* transition from the oxidized Mn species (Figure S4). With the aid of heating to push the reaction to completion, a product of the decomposition could be isolated in modest yield (Scheme 1). The byproduct was identified and characterized using single-crystal X-ray diffraction as $Mn_3(Ph_6Si_6O_{11})_2Pyr_4$ (**2,** Figure 1). The most striking feature of the resulting cluster is the loss of a $[SiOPh]^+$ unit from the **L1** trianion via the cleavage of two Si-O bonds to form a new tetraanionic ligand (Scheme 2A). This loss of a Si-O group results in a ligand that is C_{2v} symmetric, as opposed to L1, which is C_{3v} symmetric. We noted that the isolation of **2** was successful only when the introduction of O_2 was halted, and the reaction mixture was subsequently heated in pyridine. It is supposed that the oxidation of Mn^{II} to Mn^{III} in the presence of O_2 provides a more Lewis acidic metal center that facilitates heterolysis of the Si-O bonds via stabilization of the new anionic siloxide donor atoms. If O_2 addition is permitted to continue for longer (3 hours), the material is intractable. We propose complete oxidation of the Mn metals, which may lead to further Si-O heterolysis, and the formation of an impure, intractable product mixture.

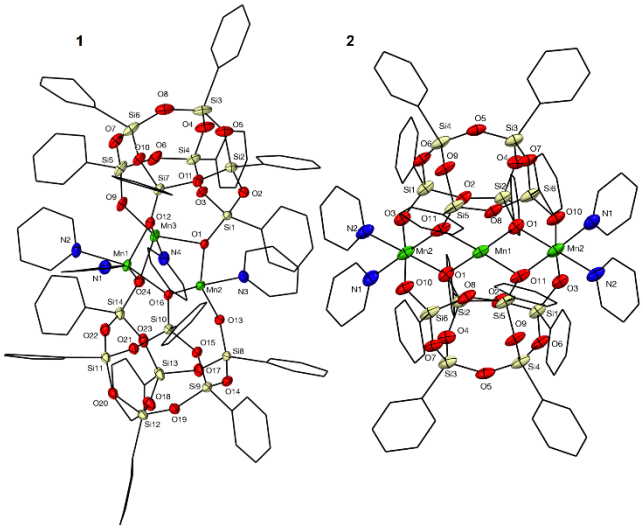

Figure 1. Crystal structure of $Mn_3(Ph_7Si_7O_{12})_2Pyr_4$ (**1**) and $Mn_3(Ph_6Si_6O_{11})_2Pyr_4$ (**2**). Ellipsoids shown at 30% probability. Carbon atoms shown as wireframe, H atoms omitted for clarity.

The Mn metal centers are now in a linear arrangement with a Mn-Mn distance of 3.0856(17) Å and the outer Mn are ligated by two pyridine solvent ligands. Charge counting considerations in **2** lead to the assignment of a formal 1-Mn^{II}:2-Mn^{III} species. Coordination geometries of the three Mn atoms permits assignment of oxidation states to specific metal ions. The bond lengths of Mn(2)-O(3)/O(10) (Table S8) are shorter (1.84-1.87 Å) in comparison to the central Mn(1) atom (2.06-2.10) and Mn(2) is in a pseudo-octahedral geometry vs the central Mn(1) in a pseudo-tetrahedral geometry. These structural features support the assignment of Mn^{III} to the exterior metal ions, and Mn^{II} to the interior. The UV/visible spectrum exhibits peaks at 437 and ~570 nm assigned as *d-d* transitions (Figure S4). The cyclic voltammogram shows a quasi-reversible reduction wave at -1.38 V vs Fc (Figure S2).

The ligand architecture in **2** has been previously observed in a few other structural reports. In one instance, an NMR-assigned structure indicated the formation of this ligand geometry upon the base-mediated hydrolytic ring opening of a trigonal prismatic $Cy_6Si_6O_9$ POSS system.[56] In a crystallographically characterized example, this ligand type formed upon the addition of MeO^- to induce the base-mediated extrusion of a $[PhSiOSiPh]^{4+}$ unit and two water molecules from a different incompletely condensed silsesquioxane, $Ph_4Si_4O_8(OH)_4$. The subsequent addition of an iron precursor resulted in the condensation of two ligand units around a hexanuclear iron cluster.[30] In another crystallographically characterized example, a pentanuclear copper cluster was self-assembled from $[PhSi(OEt)(OH)(O)]^-$

fragments in solution.[51] Both of these reported metal clusters have cores that are geometrically dissimilar from **2**.

Scheme 2. Reactions of **L1** by disruption of Si-O bond framework.

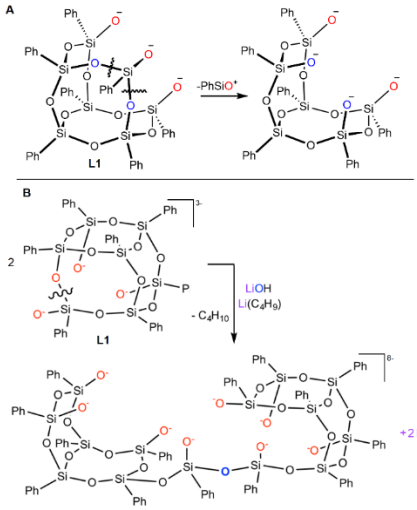

We also explored the reaction of $Mn(NR_2)_2$ with the tetradentate pro-ligand $(L2)H_4$. Only in the presence of additional 2,2'-bipyridine (Bpy) did we obtain a tractable product, $Mn_4(Ph_4Si_4O_8)_2(Bpy)_2(Py)_2$ (**3**) in good yield (Scheme 1).

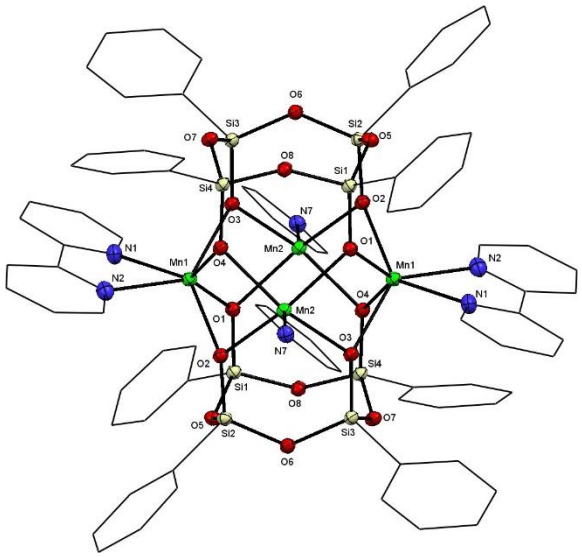

Figure 2. Crystal structure of $Mn_4(Ph_4Si_4O_8)_2(Bpy)_2(Py)_2$ (**3**). Ellipsoids shown at 30% probability. Carbon atoms shown as wireframe, H atoms and solvent omitted for clarity.

The structure of **3** (Figure 2) shows two equivalent **L2** ligands on either side of an approximately square arrangement of Mn^{II} ions. Compound **3** possesses two equivalent five-coordinate Mn(2) metal centers each with one pyridine ligand and two six-coordinate Mn(1) metal centers terminally coordinated by Bpy. Each **L2** oxygen atom bridges two Mn atoms. The Mn-Mn distances between adjacent metal centers are 3.1937(7) Å and 3.1034(7) Å. The structure type exhibited by **3** is unique among silsesquioxane ligands to our knowledge.[11] Once crystals of **3** are formed, the solid is insoluble in pyridine or THF and only slightly soluble in DMF. When the reaction was attempted without Bpy, no crystals were obtained, but instead only insoluble, amorphous solid. In addition, the reaction must be completed on a small scale (~50 mg) due to the insolubility of the resulting complex, which results in production of amorphous solid in larger scale reactions. Presumably a similar molecule forms in the absence of Bpy, but did not form a crystalline phase.

When a suspension of **3** in DMF is stirred in an O_2 atmosphere, a similar change is observed to that of **1**, and the white, cloudy suspension turns to a clear dark purple solution. A similar d-d band is observed at 465 nm along with the growth of a shoulder at 370 nm. However, we were unable to obtain crystalline products from this decomposition.

We were also able to demonstrate modifications to the **L1** ligand scaffold manganese complex by the base mediated rupture of an Si-O bond and crosslinking of two L1 units by a new oxygen atom. This O^{2-} addition was achieved via the sequential addition of LiOH and BuLi (a combination which ultimately provides a soluble equivalent of Li_2O) A sample of **1** is prepared in situ by the addition of $Mn(NR_2)_2$ to $(L1)H_3$ in a 1:1 pyridine:toluene solution. This is combined with a solution of LiOH in *N,N*-dimethylformamide (DMF), followed immediately by *n*-butyllithium in diethylether to absorb the OH proton. Subsequent crystallization using diethylether and pentane as a precipitant resulted in isolation of crystals of $Mn_3Li_2(Ph_7Si_7O_{12}OPh_7Si_7O_{12})(DMF)_5(Py)$ (**4**) (Scheme 1), which was identified with XRD. The structure of **4** (Figure 3) is asymmetric with three unique Mn^{II} metal centers. Two Li metal centers are coordinated at one side of the structure and the L1 cages are bridged via a newly formed Si-O-Si bond to form a linked pair of L1-type ligands. The Mn metal centers are in a linear arrangement and all have unique ligand environments. Mn(1) and Mn(2) are bridged to the Li metal centers, while Mn(3) is only bridged to Mn(2). It has been previously shown that the addition of base can catalyze the cleavage of the Si-O-Si moieties in the silsesquioxane cage and result in additional silanol functionalities.[56] In this reaction, the superbase *n*-butyllithium can deprotonate the LiOH, providing an oxide nucleophile to form the bridging O(13) atom between the cleaved L1 units. This transformation is illustrated in Scheme 2B. While we note that silsesquioxane rearrangement mediated by base is a known phenomenon,[30,56] **4** represents a new incompletely condensed silsesquioxane framework to our knowledge.

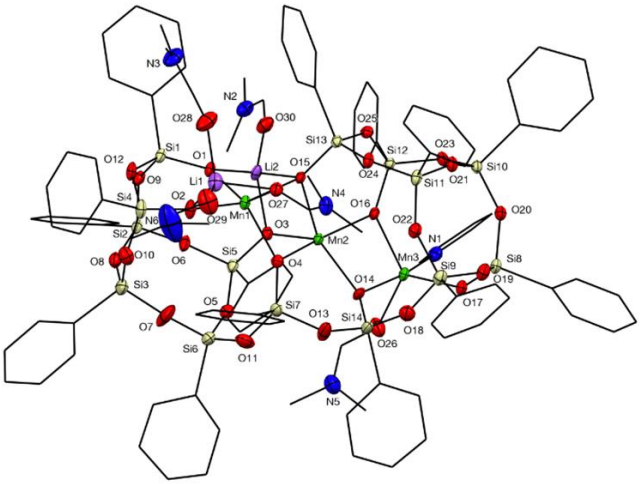

Figure 3. Crystal structure of $Mn_3Li_2(Ph_7Si_7O_{12}OPh_7Si_7O_{12})DMF_5Pyr$ (**4**). Ellipsoids shown at 30% probability. Carbon atoms shown as wireframe, H atoms and solvent omitted for clarity.

Mn-Mn distances are 3.2106(10) Å and 3.2112(10) Å. Two Mn metal centers are in distorted trigonal bipyramidal geometries and the central Mn is in a distorted square pyramidal geometry. Mn(3) is ligated by a pyridine and DMF solvent molecules, one terminal siloxide oxygen, and two μ-oxide ligands to Mn(2). Mn(2) is ligated by two μ-oxides to Mn(3) and two μ-oxides to Mn(1) in addition to a μ-oxide with Li(2) and a μ_3-oxide between Mn(1)/Mn(2) and Li(2). Mn(1) has a μ-oxide to Mn(2), a μ_3-oxide with Mn(2) and Li(2), a μ-oxide to Li(1), a neutral μ-O donor from DMF to Li(1) and a μ-oxide to Li(2).

Compound **4** was also reactive to O_2. In DMF, a solution of **4** exposed to O_2 showed the appearance of a small broad peak in the 388 and 480 nm regions, signifying *d-d* transitions, though no crystalline material was isolated. The cyclic voltammogram shows a quasi-reversible oxidation at -0.1455 V vs Fc and an irreversible reduction at -2.5695 V vs Fc (Figure S3).

In summary, four multinuclear manganese clusters templated by different silsesquioxane-derived ligand scaffolds are described. These ligands template Mn cluster complexes in varied geometric arrangements. Despite a C_{3v} symmetry in the pro-ligand $(L1)H_3$, the cluster complex of Mn(II) (**1**) is asymmetric, possessing three separate manganese environments, whereas the C_{4v} symmetric $(L2)H_4$ pro-ligand results in a nearly D_{4h} symmetric square core of manganese ions. Though the molecular symmetry is reduced to an approximate D_{2h} system by the ligation of two opposing Bpy ligands in (**3**), the ligand symmetry is more or less imposed upon the cluster complex. Similarly, upon oxidation of **1** in the presence of O_2, a ligand rearrangement results whereby a $[PhSiO]^+$ unit is extruded, giving an ostensibly C_{2v} symmetric tetroxide ligand in **2**. The resulting manganese complex retains the two fold symmetry with the metal ions rearranging into a linear trinuclear core with approximate $D_{2h,}$ symmetry. Finally, in the case of the insertion of Li_2O into the L1 scaffold, the result is cleavage of an Si-O bond and the linkage of two of the resulting fragments by oxide. While the ligand framework has, in principle, C_{2v} symmetry, the assembled pentanuclear Li_2Mn_3 cluster is asymmetric, with both lithium ions at one edge of the cluster core, and the three manganese ions forming a linear trinuclear cluster of three corner-fused rhombs, in which all atoms are environmentally unique.

ASSOCIATED CONTENT

Supporting Information. Experimental procedures, Cyclic Voltammograms, UV-absorption and FTIR spectra, and X-ray crystallographic tables, and crystallographic information files (CIF). This material is available free of charge via the Internet at http://pubs.acs.org. CIFs are also available from the CCDC under deposition numbers 2041378-2041382.

AUTHOR INFORMATION

Corresponding Author

* mzdilla@temple.edu

Present Addresses

†Department of Chemistry, University of Pennsylvania, 231 S. 34 Street, Philadelphia, PA 19104-6323

Author Contributions

The manuscript was written through contributions of all authors.

Funding Sources

NSF CHE-1800105
NSF CHE-0650456

ACKNOWLEDGMENT

The National Science Foundation under grant #1800105 is gratefully acknowledged for their support of this work. The CENTC elemental analysis center at Rochester University is supported by NSF under award number 0650456.

ABBREVIATIONS

POSS, polyhedral oligomeric silsesquioxane; XRD, X-ray Diffraction

REFERENCES

(1) Ayandele, E.; Sarkar, B.; Alexandridis, P. Polyhedral Oligomeric Silsesquioxane (POSS)-Containing Polymer Nanocomposites. *Nanomaterials* **2012,** *2*, 445-475.

(2) Feher, F. J.; Newman, D. A.; Walzer, J. F. Silsesquioxanes as models for silica surfaces. *J. Am. Chem. Soc.* **1989,** *111*, 1741-1748.

(3) Riollet, V.; Quadrelli, E. A.; Copéret, C.; Basset, J.-M.; Andersen, R. A.; Köhler, K.; Böttcher, R.-M.; Herdtweck, E. Grafting of [Mn(CH2tBu)2(tmeda)] on Silica and Comparison with Its Reaction with a Silsesquioxane. *Chem.-Eur. J.* **2005,** *11*, 7358-7365.

(4) Hanssen, Rob W. J. M.; van Santen, Rutger A.; Abbenhuis, Hendrikus C. L. The Dynamic Status Quo of Polyhedral Silsesquioxane Coordination Chemistry. *Eur. J. Inorg. Chem.* **2004,** *2004*, 675-683.

(5) Leng, Y.; Liu, J.; Zhang, C.; Jiang, P. A polyhedral oligomeric silsesquioxane (POSS)-bridged oxo-molybdenum Schiff base complex with enhanced heterogeneous catalytic activity in epoxidation. *Catal. Sci. Technol.* **2014,** *4*, 997-1004.

(6) Leng, Y.; Liu, J.; Jiang, P.; Wang, J. POSS-Derived Mesostructured Amphiphilic Polyoxometalate-based Ionic Hybrids as Highly Efficient Epoxidation Catalysts. *ACS Sustainable Chem. Eng.* **2015,** *3*, 170-176.

(7) Lu, C.-H.; Chang, F.-C. Polyhedral Oligomeric Silsesquioxane-Encapsulating Amorphous Palladium Nanoclusters as Catalysts for Heck Reactions. *ACS Catal.***2011,** *1*, 481-488.

(8) Kung, M. C.; Riofski, M. V.; Missaghi, M. N.; Kung, H. H. Organosilicon platforms: bridging homogeneous, heterogeneous, and bioinspired catalysis. *Chem. Commun.* **2014,** *50*, 3262-3276.

(9) Somorjai, G. A.; McCrea, K. R.; Zhu, J. Active Sites in Heterogeneous Catalysis: Development of Molecular Concepts and Future Challenges. *Top. Catal.* **2002,** *18*, 157-166.

(10) Al-Oweini, R.; Sartorel, A.; Bassil, B. S.; Natali, M.; Berardi, S.; Scandola, F.; Kortz, U.; Bonchio, M. Photocatalytic Water Oxidation by a Mixed-Valent MnIII3MnIVO3 Manganese Oxo Core that Mimics the Natural Oxygen-Evolving Center. *Angew. Chem. Int. Ed.* **2014,** *53*, 11182-11185.

(11) Groom, C. R.; Bruno, I. J.; Lightfoot, M. P.; Ward, S. C. The Cambridge Structural Database. *Acta Cryst. B* **2016,** *72*, 171-179.

(12) Lorenz, V.; Blaurock, S.; Edelmann, F. T. The First Heterobimetallic Metallasilsesquioxane Derivatives of Manganese. *Z. Anorg. Allg. Chem.* **2008,** *634*, 2819-2824.

(13) Ventura, M.; Mosquera, M. E. G.; Cuenca, T.; Royo, B.; Jiménez, G. Cyclopentadienyl–Silsesquioxane Titanium Complexes: Highly Active Catalysts for Epoxidation of Alkenes with Aqueous Hydrogen Peroxide. *Inorg. Chem.* **2012,** *51*, 6345-6349.

(14) Feher, F. J.; Gonzales, S. L.; Ziller, J. W. Dimeric versus monomeric titanium(III) siloxide complexes. Syntheses and characterization of [(c-C6H11)7(Si7O12)TiIII]2 and [(c-C6H11)7(Si7O12)TiIII(C5H5N)]2. *Inorg. Chem.* **1988,** *27*, 3440-3442.

(15) Crocker, M.; H. M. Herold, R.; Guy Orpen, A.; T. A. Overgaag, M. Synthesis and characterisation of titanium silasesquioxane complexes: soluble models for the active site in titanium silicate epoxidation catalysts†. *J. Chem. Soc. Dalton Trans.* **1999**, 3791-3804.

(16) Maschmeyer, T.; C. Klunduk, M.; M. Martin, C.; S. Shephard, D.; F. G. Johnson, B.; Maschmeyer, T.; Meurig Thomas, J. Modelling the active sites of heterogeneous titanium-centred epoxidation catalysts with soluble silsesquioxane analogues. *Chem. Commun.* **1997**, 1847-1848.

(17) Jones, M. D.; Davidson, M. G.; Keir, C. G.; Wooles, A. J.; Mahon, M. F.; Apperley, D. C. Heterogeneous catalysts for the controlled ring-opening polymerisation of rac-lactide and homogeneous silsesquioxane model complexes. *Dalton Trans.* **2008**, 3655-3657.

(18) Crocker, M.; H. M. Herold, R.; Crocker, M.; Guy Orpen, A. Synthesis and structural characterisation of tripodal titanium silsesquioxane complexes: a new class of highly active catalysts for liquid phase alkene epoxidation. *Chem. Commun.* **1997**, 2411-2412.

(19) Edelmann, F. T.; Gießmann, S.; Fischer, A. Silsesquioxane Chemistry, 4.: Silsesquioxane Complexes of Titanium(III) and Titanium(IV). *J. Organomet. Chem.* **2001,** *620*, 80-89.

(20) Giovenzana, T.; Guidotti, M.; Lucenti, E.; Orbelli Biroli, A.; Sordelli, L.; Sironi, A.; Ugo, R. Synthesis and Catalytic Activity of Titanium Silsesquioxane Frameworks as Models of Titanium Active Surface Sites of Controlled Nuclearity. *Organometallics* **2010,** *29*, 6687-6694.

(21) Edelmann, F. T.; Gießmann, S.; Fischer, A. A novel route to advanced model systems for silica-immobilized olefin polymerization catalysts. *Chem. Commun.* **2000**, 2153-2154.

(22) Viotti, O.; Seisenbaeva, G. A.; Kessler, V. G. Tripodal Tetrahedral Titanium Coordination in the Silica-Grafted Titania Epoxidation Catalysts: Is Not It Only a Myth? Selective Formation of [Cy7Si7O12Ti]2(μ-OR)2(μ-ROH) Cores on Thermal "Dissociation" of Alkoxytitanasilsesquioxanes. *Inorg. Chem.* **2009,** *48*, 9063-9065.

(23) Varga, V.; Pinkas, J.; Císařová, I.; Horáček, M.; Mach, K. Pentamethylcyclopentadienylmethyltitanium Silsesquioxanes and Their Zwitterionic Complexes with Tris(pentafluorophenyl)borane. *Organometallics* **2009,** *28*, 6944-6956.

(24) Masakazu, H.; Shinsuke, T.; Takashi, Y.; Keiji, U.; Masafumi, U.; Hideyuki, M. Synthesis and Structures of the First Titanium(IV) Complexes with Cyclic Tetrasiloxide Ligands: Incomplete and Complete Cage Titanosiloxanes. *Chem. Lett.* **2005,** *34*, 1542-1543.

(25) Hay, M. T.; Geib, S. J. Tetrabutylammonium isobutyl silsesquioxane monochloroferrate(III). *Acta Cryst. E* **2007,** *63*, m445-m446.

(26) Hay, M. T.; Geib, S. J.; Pettner, D. A. Aerobic oxidation of tetrahydrofuran by a series of iron (III) containing POSS compounds. *Polyhedron* **2009,** *28*, 2183-2186.

(27) Hay, M. T.; Hainaut, B. J.; Geib, S. J. Synthesis and characterization of a novel iron (III) silsesquioxane compound. *Inorg. Chem. Commun.* **2003,** *6*, 431-434.

(28) Lorenz, V.; Fischer, A.; Edelmann, F. T. Erstmaliger Einbau eines späten Übergangsmetalls in ein Silsesquioxan-Gerüst: Synthese und strukturelle Charakterisierung von Cy7Si7O12Fe(tmeda). *Z. Anorg. Allg. Chem.* **2000,** *626*, 1728-1730.

(29) Liu, F.; John, K. D.; Scott, B. L.; Baker, R. T.; Ott, K. C.; Tumas, W. Synthesis and Characterization of Iron Silasesquioxane Phosphane Complexes. *Angew. Chem. Int. Ed.* **2000,** *39*, 3127-3130.

(30) Manicke, N.; Hoof, S.; Keck, M.; Braun-Cula, B.; Feist, M.; Limberg, C. A Hexanuclear Iron(II) Layer with Two Square-Planar FeO4 Units Spanned by Tetrasiloxide Ligands: Mimicking of Minerals and Catalysts. *Inorg. Chem.* **2017,** *56*, 8554-8561.

(31) Pinkert, D.; Demeshko, S.; Schax, F.; Braun, B.; Meyer, F.; Limberg, C. A Dinuclear Molecular Iron(II) Silicate with Two High-Spin Square-Planar FeO4 Units. *Angew. Chem. Int. Ed.* **2013,** *52*, 5155-5158.

(32) Ohde, C.; Limberg, C.; Schmidt, D.; Enders, M.; Demeshko, S.; Knispel, C. Progress in the Compilation of an Oxovanada-Silsesquioxane Portfolio and Catalytic Activity of Organometallic Representatives in Ethylene Polymerisation. *Z. Anorg. Allg. Chem.* **2010,** *636*, 2315-2322.

(33) Ohde, C.; Limberg, C.; Stösser, R.; Demeshko, S. Oxovanadium(IV) Silsesquioxane Complexes. *Inorg. Chem.* **2010,** *49*, 2479-2485.

(34) Ohde, C.; Brandt, M.; Limberg, C.; Döbler, J.; Ziemer, B.; Sauer, J. V2O5/SiO2 surface inspired, silsesquioxane-derived oxovanadium complexes and their properties. *Dalton Trans.* **2008**, 326-331.

(35) Feher, F. J.; Walzer, J. F. Synthesis and characterization of vanadium-containing silsesquioxanes. *Inorg. Chem.* **1991,** *30*, 1689-1694.

(36) Ohde, C.; Limberg, C. From Surface-Inspired Oxovanadium Silsesquioxane Models to Active Catalysts for the Oxidation of Alcohols with O2—The Cinnamic Acid/Metavanadate System. *Chem.-Eur. J.* **2010,** *16*, 6892-6899.

(37) Feher, F. J.; Walzer, J. F. Antiferromagnetic exchange in an isomorphous series of siloxy-bridged early-transition-metal dimers: comparisons of antiferromagnetic exchange interactions in isomorphous d1-d1, d1-d2, d2-d2, and d2-d3 exchange-coupled dimers. *Inorg. Chem.* **1990,** *29*, 1604-1611.

(38) Jones, M. D.; Keir, C. G.; Johnson, A. L.; Mahon, M. F. Crystallographic characterisation of novel Zn(II) silsesquioxane complexes and their application as initiators for the production of polylactide. *Polyhedron* **2010,** *29*, 312-316.

(39) Duchateau, R.; van Meerendonk, W. J.; Huijser, S.; Staal, B. B. P.; van Schilt, M. A.; Gerritsen, G.; Meetsma, A.; Koning, C. E.; Kemmere, M. F.; Keurentjes, J. T. F. Silica-Grafted Diethylzinc and a Silsesquioxane-Based Zinc Alkyl Complex as Catalysts for the Alternating Oxirane−Carbon Dioxide Copolymerization. *Organometallics* **2007,** *26*, 4204-4211.

(40) Schax, F.; Braun, B.; Limberg, C. A Tripodal Trisilanol Ligand and Its Complexation Behavior towards CuI, CuII, and ZnII. *Eur. J. Inorg. Chem.* **2014,** *2014*, 2124-2130.

(41) Ovchinnikov, Y. E.; Shklover, V. E.; Struchkov, Y. T.; Levitsky, M. M.; Zhdanov, A. A. Synthesis and crystal structure of the salt Na6[(PhSiO1.5)2Co3O6]·7H2O containing a cobaltasiloxane anionic framework. *J. Organomet. Chem.* **1988,** *347*, 253-267.

(42) Ehle, S.; Brüser, V.; Lorenz, V.; Hrib, C. G.; Saulich, K.; Müller, S.; Quade, A.; Edelmann, F. T. Linear Heterometallic Co3Li2 and Co4Li2 Siloxides: Precursors for the Plasma Synthesis of Adsorbent Materials. *Eur. J. Inorg. Chem.* **2013,** *2013*, 1451-1457.

(43) Werndrup, P.; Kessler, V. G. Bis-silsesquioxane complex as a molecular model of transition metal oxide–zeolite nanocomposite. *Inorg. Chem. Commun.* **2004,** *7*, 588-591.

(44) Bilyachenko, A. N.; Yalymov, A. I.; Korlyukov, A. A.; Long, J.; Larionova, J.; Guari, Y.; Zubavichus, Y. V.; Trigub, A. L.; Shubina, E. S.; Eremenko, I. L.et al. Heterometallic Na6Co3

Phenylsilsesquioxane Exhibiting Slow Dynamic Behavior in its Magnetization. *Chem.-Eur. J.* **2015,** *21*, 18563-18565.

(45) Liu, Y.-N.; Su, H.-F.; Li, Y.-W.; Liu, Q.-Y.; Jagličić, Z.; Wang, W.-G.; Tung, C.-H.; Sun, D. Space Craft-like Octanuclear Co(II)-Silsesquioxane Nanocages: Synthesis, Structure, Magnetic Properties, Solution Behavior, and Catalytic Activity for Hydroboration of Ketones. *Inorg. Chem.* **2019,** *58*, 4574-4582.

(46) Schax, F.; Bill, E.; Herwig, C.; Limberg, C. Dioxygen Activation by Siloxide Complexes of Chromium(II) and Chromium(IV). *Angew. Chem. Int. Ed.* **2014,** *53*, 12741-12745.

(47) Feher, F. J.; Blanski, R. L. Polyhedral oligometallasilasesquioxanes as models for silica-supported catalysts: chromium attached to two vicinal siloxy groups. *J. Chem. Soc., Chem. Commun.* **1990**, 1614-1616.

(48) Bilyachenko, A. N.; Korlyukov, A. A.; Vologzhanina, A. V.; Khrustalev, V. N.; Kulakova, A. N.; Long, J.; Larionova, J.; Guari, Y.; Dronova, M. S.; Tsareva, U. S.et al. Tuning linkage isomerism and magnetic properties of bi- and tri-metallic cage silsesquioxanes by cation and solvent effects. *Dalton Trans.* **2017,** *46*, 12935-12949.

(49) Bilyachenko, A. N.; Dronova, M. S.; Yalymov, A. I.; Korlyukov, A. A.; Shul'pina, L. S.; Arkhipov, D. E.; Shubina, E. S.; Levitsky, M. M.; Kirilin, A. D.; Shul'pin, G. B. Binuclear Cage-Like Copper(II) Silsesquioxane ("Cooling Tower") – Its High Catalytic Activity in the Oxidation of Benzene and Alcohols. *Eur. J. Inorg. Chem.* **2013,** *2013*, 5240-5246.

(50) Edelmann, F. T.; Gießmann, S.; Fischer, A. Silsesquioxane Chemistry, 5. Retention of the Cu4O4 core upon formation of the first copper(I) silsesquioxane from tetrameric copper(I)-t-butoxide. *Inorg. Chem. Commun.* **2000,** *3*, 658-661.

(51) Astakhov, G. S.; Levitsky, M. M.; Korlyukov, A. A.; Shul'pina, L. S.; Shubina, E. S.; Ikonnikov, N. S.; Vologzhanina, A. V.; Bilyachenko, A. N.; Dorovatovskii, P. V.; Kozlov, Y. N.et al. New Cu4Na4- and Cu5-Based Phenylsilsesquioxanes. Synthesis via Complexation with 1,10-Phenanthroline, Structures and High Catalytic Activity in Alkane Oxidations with Peroxides in Acetonitrile. *Catalysts* **2019,** *9*, 701.

(52) Bilyachenko, A. N.; Kulakova, A. N.; Levitsky, M. M.; Petrov, A. A.; Korlyukov, A. A.; Shul'pina, L. S.; Khrustalev, V. N.; Dorovatovskii, P. V.; Vologzhanina, A. V.; Tsareva, U. S.et al. Unusual Tri-, Hexa-, and Nonanuclear Cu(II) Cage Methylsilsesquioxanes: Synthesis, Structures, and Catalytic Activity in Oxidations with Peroxides. *Inorg. Chem.* **2017,** *56*, 4093-4103.

(53) Lorenz, V.; Fischer, A.; Edelmann, F. T. Silsesquioxane chemistry.: Part 10. Silsesquioxane silanolate complexes of samarium and scandium. *J. Organomet. Chem.* **2002,** *647*, 245-249.

(54) Winkhofer, N.; Roesky, H. W.; Noltemeyer, M.; Robinson, W. T. [tBuSiO(ReO4)]4, a Model Compound for Metal Oxides on Silicate Surfaces—Synthesis from the Stable Triol tBuSi(OH)3 and Re2O7. *Angew. Chem. Int. Ed. in English* **1992,** *31*, 599-601.

(55) Andersen, R. A.; Faegri, K.; Green, J. C.; Haaland, A.; Lappert, M. F.; Leung, W. P.; Rypdal, K. Synthesis of bis[bis(trimethylsilyl)amido]iron(II). Structure and bonding in M[N(SiMe3)2]2 (M = manganese, iron, cobalt): two-coordinate transition-metal amides. *Inorg. Chem.* **1988,** *27*, 1782-1786.

(56) J. Feher, F.; Terroba, R.; W. Ziller, J. Base-catalyzed cleavage and homologation of polyhedral oligosilsesquioxanes. *Chem. Commun.* **1999**, 2153-2154.

For Table of Contents Only

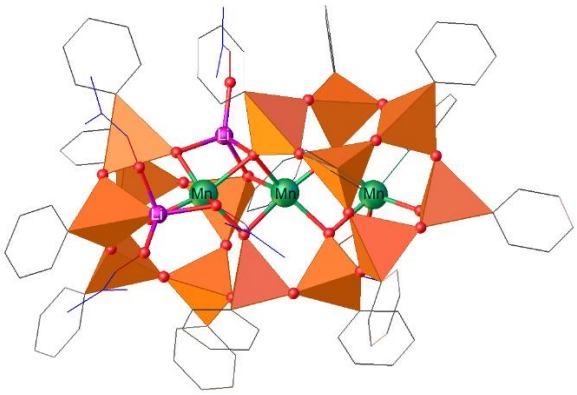

A series of manganese and lithium-manganese complexes templated by ligand derivatives of polyhedral oligomeric silsesquioxane (POSS) are described. We describe Si-O bond rupture and formation to fragment or join silsesquioxane ligands. Above is shown an asymmetric Li_2Mn_3 cluster templated by a large octanuclear silsesquioxane ligand formed by linkage of two smaller ligands. SiO_3C tetrahedra are shown in orange.